Am J Cancer Res 2026;16(3):1013-1026
www.ajcr.us /ISSN:2156-6976/ajcr0171372

Original Article

Epigenetic reprogramming of hexokinase domain containing 1 (HKDC1) promotes proliferation in colorectal cancer

Kuo-Hsing Chen[1,2,3], Liang-Chuan Lai[4], Liang-In Lin[5,6], Chia-Lang Hsu[3,7,8], Yi-Hsin Liang[2,3], Been-Ren Lin[9], Ann-Lii Cheng[1,2,3], Eric Y. Chuang[10,11], Kun-Huei Yeh[2,3]

[1]Department of Medical Oncology, National Taiwan University Cancer Center, Taipei, Taiwan; [2]Department of Oncology, National Taiwan University Hospital, Taipei, Taiwan; [3]Graduate Institute of Oncology, National Taiwan University College of Medicine, Taipei, Taiwan; [4]Graduate Institute of Physiology, National Taiwan University College of Medicine, Taipei, Taiwan; [5]Department of Laboratory Medicine, National Taiwan University Hospital, Taipei, Taiwan; [6]Department of Clinical Laboratory Sciences and Medical Biotechnology, National Taiwan University College of Medicine, Taipei, Taiwan; [7]Department of Medical Research, National Taiwan University Hospital, Taipei, Taiwan; [8]Graduate Institute of Medical Genomics and Proteomics, National Taiwan University College of Medicine, Taipei, Taiwan; [9]Department of Surgery, National Taiwan University Hospital, Taipei, Taiwan; [10]Bioinformatics and Biostatistics Core, Center of Genomic and Precision Medicine, Taipei, Taiwan; [11]Graduate Institute of Biomedical Electronics and Bioinformatics, National Taiwan University, Taipei, Taiwan

Received January 10, 2026; Accepted March 16, 2026; Epub March 25, 2026; Published March 30, 2026

Abstract: Dysregulation of cellular metabolism is one of the hallmarks of cancer. Tumor cells would enhance glycolysis to fuel the phenotypes of rapid proliferation and invasion. This study aims to explore epigenetic reprogramming of glycolysis pathway in colorectal cancer (CRC). CRCs and the adjacent normal colon tissues were profiled by using a comprehensive methylation array (Illumina Methylation EPIC Beadchips) to comprehensively analyze the methylation alterations in the glycolysis pathway. Differentially methylated genes (DMGs) were identified by using β value difference (≥ 0.2 or ≤ -0.2) and Wilcoxon rank-sum test ($P < 0.05$), and the common DMG in open datasets (GSE42752, GSE25062 and TCGA). Pyrosequencing was executed to validate the DMGs. Hexokinase domain containing 1 (*HKDC1*), the major hypomethylated gene we found, was overexpressed in colon cancer cells. Cells were treated with an HKDC1 inhibitor to elucidate the role of *HKDC1*. We found hypomethylation of *HKDC1* was the only shared hypomethylated DMG in glycolysis pathway after comparing our methylation profiles of CRC to 3 public datasets. The RT-qPCR study in our cohort and the negative association between mRNA expression of *HKDC1* and methylation status in TCGA dataset support *HDKC1* expression is methylation-regulated. Overexpression of *HKDC1* in colon cancer cells resulted in increased proliferation of colon cancer cells and decreased cytotoxicity by an HKDC1 inhibitor. RNA sequencing revealed significant up-regulation of glycolysis, cell cycle, E2F, and its targets in *HKDC1* overexpressed cells. In summary, hypomethylation of *HKDC1* is common in CRC and may regulate cellular metabolism to promote proliferation of colon cancer cells through upregulation of glycolysis and cell cycle pathways.

Keywords: Colorectal cancer, HKDC1, cancer metabolism, epigenetics, glycolysis, cell cycle

Introduction

The incidence of colorectal cancer (CRC) has been increasing globally in the past three decades, and the number of newly diagnosed patients in 2020 was 1.9 million, which is the third cancer in terms of incidence [1]. CRC has also been the leading cancer in newly diagnosed patients for more than 10 years in Taiwan, with an age-standardized incidence rate of 62.0 (48.9-80.0) per 100,000 in 2019 [2]. Generally, an increased Westernized diet, high body mass index (BMI), metabolic syndrome, and sedentary lifestyle are recognized as risk factors for CRC [3-5]. Among these, high BMI, high waist circumference, and decreased physical activity are indicators of energy balance.

https://doi.org/10.62347/OSSN5233

Dysregulation of cellular metabolism is an emerging hallmark of cancer [6]. It is becoming increasingly clear that there must be a corresponding adjustment in cellular metabolism to fuel the phenotypes of rapid proliferation and invasion in cancers. The Warburg effect is probably the most prevalent and well-known metabolic change associated with cancer cells [7]. Cancer cells have enhanced glucose metabolism via glycolysis to generate lactate (which can generate two ATPs for each molecule of glucose) instead of oxidative phosphorylation (which can generate 36 ATPs for each molecule of glucose), even if oxygen levels are normal. Although this process is less efficient in ATP generation, glycolysis is much faster and glycolysis intermediates are essential for macromolecular biosynthesis and redox homeostasis [8].

Several mechanisms regulate the metabolic genes in cancer cells to fuel their growth. Oncogenic mutations play a well-known role in metabolic rewiring in human cancers. For example, *KRAS, PIK3CA, Akt or PTEN* have been shown to activate *Akt-mTOR* pathway, which leads to glycolysis stimulation via the phosphorylation of hexokinase, the rate-limiting enzyme in glycolysis, and the upregulation of glucose transporter 1 (*GLUT1*), a key gene involved in shuttling glucose into cells [9-11]. On the other hand, epigenetic reprogramming of metabolic genes expression also has been shown to play an important role in dysregulation of metabolism in cancer. Epigenetics refers to heritable changes in gene expression without alterations in DNA sequences. For example, DNA methylation in promoter or enhancer regions can regress gene expression by recruiting proteins that induce changes in chromatin accessibility and interfere with transcription factor binding [12]. A previous study showed that DNA methylation mediates epigenetic loss of *Derline-3,* a key gene involved in the proteasomal degradation of *GLUT1*, and leads to overexpression of *GLUT1* [13]. Hypermethylation of the pyruvate kinase isoform 2 (*PKM2*) has also been reported in multiple cancer types [14]. *PKM2* is the predominant isoform in proliferating cells and drives glucose flux for macromolecule biosynthesis.

In the Dutch Hunger Winter study, by analyzing residents who experienced World War II, strict energy restriction during early life has been shown to be associated with a decreased incidence of CRC [15]. On the other hand, a genome-wide methylation analysis of whole blood in two groups of baboons with different resource bases (wild feeding and lodge environment) revealed that the largest differentially methylated regions identified after famine were in the promoter region of a key glycolysis-related gene, phosphofructokinase platelet *(PFKP)* [16]. Given that many risk factors for CRC are indicators of energy balance, and epigenetic regulation of gene expression can be very plastic and responsive to environmental stress [17], we hypothesized that epigenetic reprogramming of the glycolysis pathway increases cancer energy metabolism and promotes CRC development.

Materials and methods

Primary tumor samples

This study aimed to explore epigenetic reprogramming of the glycolysis pathway in CRC. Primary CRC tumor samples were obtained from a prospective CRC cohort and collected during clinically indicated surgical procedures [18]. The adjacent normal colonic mucosa tissue was collected from resected unaffected parts of the colon located approximately at least 5 cm away from the tumor location in the same cohort. Patients were eligible to participate in this study if they met the following inclusion criteria: (1) pathology-confirmed CRC, (2) age ≥ 20 years old or older, and (3) history of colectomy. Informed consent was obtained from CRC tumors and adjacent normal colon specimens. Patients were excluded if they had received chemotherapy or radiotherapy for CRC prior to tumor sample collection. The patients' clinicopathological characteristics, such as age, sex, histology, tumor stage, primary tumor site (designated as the left-sided colon if located from the descending colon to the rectum, and the right-sided colon if located from the cecum to the splenic flexure), BMI, etc. were collected [18]. All patients provided informed consent before enrolling in this prospective study. The study was approved by the Institutional Review Board of National Taiwan University Hospital (approval number: 201712132RINA). All procedures performed in studies involving human participants were in

accordance with the ethical standards of the institutional and/or national research committee and with the 1964 Helsinki Declaration and its later amendments or comparable ethical standards.

Methylation array and pyrosequencing

Genomic DNA was extracted from fresh frozen CRC tumors and adjacent normal colonic mucosa specimens using proteinase K-phenol-chloroform extraction following standard protocols with 0.5% SDS and 200 μg/ml proteinase K. DNA quantification was performed using Nanodrop (Thermo Fisher, Waltham, MA, USA). A normalized DNA concentration of 50 ng/μl and total genomic DNA (500 ng) were used for bisulfite conversion using the EZ DNA Methylation Kit (Zymo Research, Irvine, CA, USA) and 200 ng of bisulfate treated DNA was used for the Infinium MethylationEPIC Assay (Illumina, San Diego, CA, USA). The bisulfate-converted DNA was amplified by DNA polymerase during the incubation step in an Illumina Hybridization Oven for 20-24 hours at 37°C. The amplified DNA product was fragmented into 300-600 base pairs. After alcohol precipitation and resuspension of the fragmented DNA, the BeadChip was prepared for hybridization in the capillary flow-through chamber (Illumina Human MethylationEPIC BeadChip Array, Illumina, San Diego, CA, USA). The amplified and fragmented DNA samples were annealed to locus-specific 50-mers during the hybridization step at 48°C for 16 h in an Illumina Hybridization Oven. After hybridization, allelic specificity was determined using enzymatic single-base extension. The products were subsequently fluorescently stained with biotin-ddNTPs or dinitrophenol-ddNTPs. The intensities of the bead fluorescence were detected by the Illumina HiScan (iScan Control Software v.3.3.28), and the results were analyzed using GenomeStudio v2011.1 software for methylation profiles.

The processed methylation chips were sent to a HiScan reader (Illumina, San Diego, CA, USA) for scanning. Then, 27 CRC tumors and 5 adjacent normal colonic mucosa samples were processed on the same chip, and all samples were processed at the same time to avoid variation from chip-to-chip.

Preprocessing and data quality control of the EPIC array were conducted using the R package minfi, which facilitates background correction, normalization, and probe filtering. During preprocessing, minfi computed the detection *P*-value by comparing the total signal intensity (sum of methylated and unmethylated signals) of each probe to the background noise, typically estimated from negative control probes. Probes with lower detection *p*-values were considered to have higher signal fidelity. Samples with an average detection *P*-value greater than 0.05 were excluded from further analysis as part of sample-level quality control. Following sample filtering, functional normalization was applied to correct for unwanted technical variations. This method integrates the Noob algorithm for background adjustment while leveraging covariates derived from control probes to mitigate batch effects and systematic biases. By applying this strategy, global technical variability across samples was reduced without making prior distributional assumptions. The effectiveness of normalization was assessed by examining the distribution of beta values, with outlier samples exhibiting substantial deviations flagged for potential exclusion in downstream analyses. For probe-level quality control, we implemented a filtering step to remove two specific categories of probes: (1) those with an average detection *P*-value exceeding 0.05, (2) those located on sex chromosomes, (3) those affected by SNPs, and (4) those showing cross-reactivity. To validate dataset integrity, multidimensional scaling plots from principal component analysis were generated to examine sample clustering patterns, ensuring that observed methylation differences accurately reflected biological variability between groups. The methylation intensities were transformed into β values.

Pyrosequencing analysis was performed using a PyroMark Q24 (QIAGEN, USA). EpiTect® Control DNA (QIAGEN) (0% unmethylated control and 100% methylated control) was used as the control. The primer sequences were as followings. For cg11639651, the PCR amplification primers were AGTTTGGGATTGGAAATTTGTAGAG (F1) and Biotin-ACTTAAAAATTAAATACCACCAAATCTCAT (R1), and the sequencing primer was ATTGGAAATTTGTAGAGTAG (S1). For cg11762346, the PCR amplification primers were GTGGGGGGGAGTTTAATTATTGA (F2) and

Biotin-CTTAATCTAATCCTCCTTCAACTTAC (R2), and the sequencing primer was AGGTTGGAGGTATTTAG (S1). Quantitation of cytosine methylation as done using PyroMark Q24 Software.

Real-time quantitative polymerase chain reaction

Total RNA was extracted from fresh frozen CRC tumors and adjacent normal colon tissues using the RNeasy Isolation Kit, and RNA quantity and integrity were evaluated using a bioanalyzer (Agilent Technologies, Palo Alto, CA). Real-time quantitative polymerase chain reaction (RT-qPCR) was performed on an Applied Biosystems™ 7900HT Fast Real-Time PCR System using TaqMan Fast Advanced Master Mix with TaqMan probes. Data were analyzed using the $2^{-\Delta\Delta Ct}$ method and normalized to the amount of glyceraldehyde-3-phosphate dehydrogenase (GAPDH) mRNA. TaqMan probes used for RT-qPCR analysis were GAPDH (Hs02-786624_g1), hexokinase domain containing 1 (HKDC1) (Hs00228405_m1), and Aldehyde Dehydrogenase 1 Family Member A3 (ALDH1-A3) (Hs00167476_m1) (Applied Biosystems, Waltham, MA, USA). The experiments were performed for three times in triplicate.

Cell lines and compounds

The human CRC cell lines COLO320DM and SW480 were obtained from the American Type Culture Collection (Rockville, MD, USA). Cells were maintained in RPMI-1640 containing 10% fetal bovine serum, 2 mmol/L L-glutamine (Life Technologies, Carlsbad, CA, USA), PSA (10,000 units/ml penicillin, 10 mg/ml mg/mL streptomycin, and 25 μg/ml amphotericin B; Biological Industries, Kibbutz Beit Haemek, Israel). The cells were cultured at 37°C in a humidified incubator containing 5% CO_2.

NSC24500 (2,6-dimethoxy-1,4-benzoquinone) was purchased from Sigma-Aldrich (St. Louis, MO). NSC24500 was active in HK5 (an alternative name of HKDC1) assay (half maximal inhibitory concentration or IC_{50} = 2.49 μM, BioAssay AID: 504729; IC_{50} = 3.54 μM, BioAssay AID: 504763) in PubChem (https://pubchem.ncbi.nlm.nih.gov/compound/68262#section=Biological-Test-Results).

HKDC1 transfection

pCMV6-HKDC1 (RC221178) and pCMV6-Entry vectors were purchased from OriGene Technologies (Rockville, MD, USA). Transfection was performed in Opti-MEM™ (Gibco) using a mix containing Lipofectamine 2000 (Invitrogen, Carlsbad, CA, USA) and 10 μg plasmid, for 24 h at 37°C and 5% CO_2. The Transfection was stopped after 24 h by replacing the medium containing the plasmid with standard medium in which the cells were routinely cultured. Transfection was validated by HKDC-1 expression in protein lysates.

Antibodies and western blots

COLO320DM and SW480 cells transiently transfected with pCMV6-HKDC1 and pCMV6-Entry Vector and SW480 cells treated with NSC24500 were collected and lysed with RIPA lysis buffer (50 mmol/L Tris-HCl [pH 8.0], 150 mmol/L NaCl, 1% NP40, 0.5% sodium deoxycholate, 0.1% SDS). The Pierce BCA protein assay (Thermal Scientific, Odessa, Texas, USA) was used to determine the protein concentration of the cell lysate. Briefly, 20 mg of protein per lane was separated by 8% (w/v) sodium dodecyl sulfate polyacrylamide gel electrophoresis (SDS-PAGE) and transferred to a polyvinylidene fluoride membrane (Millipore, Bedford, MA, USA). Membranes were blocked with 5% (w/v) bovine serum albumin. After washing with Tris-buffered saline containing 0.1% Tween buffer, the membranes were incubated overnight at 4°C with primary antibodies. The primary antibodies included anti-HKDC-1 (1:3000; Sigma-Aldrich, St. Louis, MO, USA), anti-DDK (1:1000; OriGene Technology, Rockville, MD, USA), and anti-GAPDH (1:50000; Cell Signaling, Denver, LA, USA). After washing with PBST three times, the membranes were incubated with horseradish peroxidase-conjugated anti-rabbit (1:5000) and anti-mouse (1:5000) antibodies at temperature for 1 h and protein bands were visualized using an ECL kit (Merck, Millipore, USA) with GAPDH as an internal control.

Cell viability assay

Colo320DM and SW480 cell viability assays were performed using the MTT assay (Tokyo Chemical Industry Inc., Tokyo, Japan) with at least three replicates. Cells were seeded in 96-well plates at densities of 2×10^3 cells and 1×10^3 cells per well and cultured in RPMI medium for 24, 72, 120, and 168 h, respectively. At each time point, cells were incubated with 50 ml 3-(4,5-dimethylthiazol-2-yl)-2,5-diphenyltet-

razolium bromide (final concentration 0.5 mg/ml) at 37°C for 2 h. After incubation, the medium was removed, DMSO (200 μl per well) was added to end the reaction, and the absorbance was determined using an ELISA plate reader at 540 nm at the indicated time. IC_{50} was determined using Calcusyn software (CalcuSyn Version 2.0, Norway).

RNA sequencing and library preparation

Total RNA was extracted using Tri Reagent (Ambion, Austin, TX, USA), and the RNA concentration and quality were evaluated using a NanoDrop ND-1000 spectrophotometer (Thermo Scientific, Wilmington, USA) and an Agilent 2100 Bioanalyzer (Agilent Technologies, Palo Alto, CA). Total RNA with A260/A280 = 1.8-2.0 and RNA integrity number > 8.0, were used for further experiments. We normalized intact RNA samples to 200 ng/μl with DEPC-treated H_2O, and then total RNA (1-2 μg) was purified using poly T oligo-attached magnetic beads. Following purification, mRNA was fragmented into small pieces using divalent cations at elevated temperatures. Cleaved RNA fragments were copied into first-strand cDNA using reverse transcriptase and random primers. This was followed by second-strand cDNA synthesis using DNA polymerase I and RNaseH. These cDNA fragments then go through an end repair process, the addition of a single "A" base, and ligation of the adapters. The products were purified and enriched using PCR to create the final cDNA library. Paired-end 150 nucleotide reads from each cDNA library were obtained using NovaSeq6000 (Illumina Inc. San Diego, CA, USA).

RNA-sequencing data analysis

Trimmomatic [19] was used to assess the quality of raw reads, including duplication, k-mer, and GC content levels. Outliers with > 30% disagreement were discarded. Raw reads were mapped onto the human genome using hisat [20]. More than 80% of the mapped reads were retained for further analyses. The read count matrix was normalized across all samples using the TMM method and converted into transcripts per million (TPMs) for further analysis. Pre-ranked gene-set enrichment analysis (GSEA) was performed using the function implemented by the R package clusterProfiler on the gene sets from MSigDB (v7.4). The genes were ranked based on the score of sign (log2FC) *-log10 (*p*-value), where log2FC and *p*-value were obtained by performing differential expression analysis using the R package limma procedure.

Statistical analysis

For the methylation array, the methylation level of CpG loci was calculated as β-values (β = intensity (methylated)/intensity (methylated + unmethylated)). Correlation coefficient and principal component analysis (PCA) were performed for quality control. The Wilcoxon rank-sum test was used for statistical tests. Statistical analyses of RNA-seq data were performed using R language. For *in vivo* studies, all data were repeated in at least three independent experiments. Quantitative data are represented as mean +/- SD standard deviation (SD). Data from the same experiments were compared using Student's t-test. Statistical significance was set at $P < 0.05$. The Benjamini-Hochberg procedure was applied to control the false discovery rate in the differential expression analysis.

Results

To explore the epigenetic deregulation of glycolysis in CRC, genome-scale analysis of DNA methylation was conducted in 27 CRC tumors and 5 adjacent normal colon samples using Illumina Methylation EPIC Beadchips. The clinicopathological features of these CRC patients are shown in **Table 1**. Wilcoxon rank-sum test ($P < 0.05$) and β value difference (≥ 0.25 or ≤ -0.25) were used to evaluate the methylation differences between CRC tumors and adjacent normal colon samples. Of these, 7,672 differentially methylated genes (DMGs) were found between 27 CRCs tumors and 5 adjacent normal colons. PCA demonstrated a distinct cluster of adjacent normal colon and CRC tumor samples (**Figure 1**). When we focused on glycolysis pathway (defined by KEGG pathway, N = 67), we identified 17 hypomethylation genes (25%) and 2 hypermethylation genes (3%) that are involved in glycolysis pathway genes in CRC (**Table 2**).

Next, our findings were compared with the other 3 datasets (focused on glycolysis pathway genes) from Russian (GSE42752), Netherlands and Canada (GSE25062), and TCGA, and we identified hypomethylation of hexokinase

Table 1. Clinicopathologic characteristics of patients

Characteristic	Number (%)
Age at diagnosis (years)	
< 50	9 (33)
50-70	10 (37)
> 70	8 (30)
Sex	
Male	16 (59)
Female	11 (41)
Stage	
1-3	22 (82)
4	5 (18)
Location of primary tumor	
Left-sided	22 (82)
Right-sided	5 (18)
Body mass index	
< 25	18 (67)
≥ 25	9 (33)
Diabetes mellitus	
Yes	9 (33)
No	2 (3.7)

domain containing 1 (*HKDC1*) (2 loci: cg11639651, cg11762346) and hypermethylation of aldehyde dehydrogenase 1 family member A3 (*ALDH1A3*) (2 loci: cg21359747, cg27652350) across all four datasets when evaluating with a β value difference ≥ 0.2 or ≤ -0.2 [21-23]. To validate the findings from the methylation array, pyrosequencing was performed to evaluate the methylation status of *HKDC1* and *ALDH1A3* in the same specimens sent for the methylation array EPIC study. The results showed that the methylation patterns of these specimens were similar in the pyrosequencing and methylation arrays (**Figure 2**; Supplementary Table 1). qRT-PCR experiments were performed to evaluate the expression of *HKDC1* and *ALDH1A3* in 27 CRC tumors and five adjacent normal colons that were tested in the methylation array. However, there were no residual specimens in the five adjacent normal colons and 10 of 27 CRC tumors; thus, qRT-PCR was performed in the other 17 of 27 CRC tumors and 14 of 27 CRC adjacent normal colons. The results showed that there was significantly higher gene expression of *HKDC1* (P = 0.01) in CRC tumors than in adjacent normal colons, while the gene expression of *ALDH1A3* was similar between CRC tumors and adjacent normal colon tissues (P = 0.20) (**Figure 3**). These data suggest that hypomethylation of *HKDC1* in CRC tumors relative to adjacent normal colons is associated with higher gene expression of *HKDC1* in CRC tumors than in adjacent normal colons. However, this relationship was not observed in *ALDH1A3*. We investigated the HKDC1 methylation by pyrosequencing and the mRNA expression by qPCR in 6 colon cancer cell lines (COLO205, COLO320, SW480, SW620, HCT15, and HT29). We found there was significantly strong negative correlation between HKDC1 methylation based on two loci (cg11762346 and cg11639651) and HKDC1 mRNA expression (Pearson's correlation coefficient = -0.95, P = 0.004 for cg11762346 and Pearson's correlation coefficient = -0.96, P = 0.002 for cg11639651) (Supplementary Table 2 and Supplementary Figure 1). Next, we searched the open data in cBioPortal for Cancer Genomics (TCGA, Firehose Legacy) and found a negative correlation between gene expression and DNA methylation in *HKDC1* (Pearson's correlation coefficient = -0.43, P = $9.48e^{-18}$) in CRC (**Figure 4**). The above results further support that the gene expression of *HKDC1* in CRC is methylation-regulated.

Because the basal expression of HKDC1 in COLO320DM and SW480 cells was not abundant (Supplementary Figure 2), we overexpressed *HKDC1* in COLO320DM and SW480 cells to explore the biological effect of HKDC1 on cell proliferation and did not perform *HKDC1* knockdown experiments. The expression of *HKDC1* was increased after *HKDC1* overexpression, and the proliferation of COLO320DM and SW480 cells was significantly increased in *HKDC1*-transfected cells compared to that in the negative control group (**Figure 5**). An additional power-point file shows this in more detail (see Supplementary Figure 3). Next, SW480 cells were treated with an HKDC1 inhibitor (NSC24500), with or without *HKDC1* overexpression. The data revealed that *HKDC1* overexpression mitigated the cytotoxic effects of NSC24500 (**Figure 6**). The above studies suggested *that HKDC1* could promote the proliferation of colon cancer cells.

Next, we performed RNA sequencing in COLO320DM and SW480 cells after pCMV6-HKDC1 or pCMV6-entry transfection to explore gene expression that could potentially contribute to promoting cell proliferation. PCA revealed

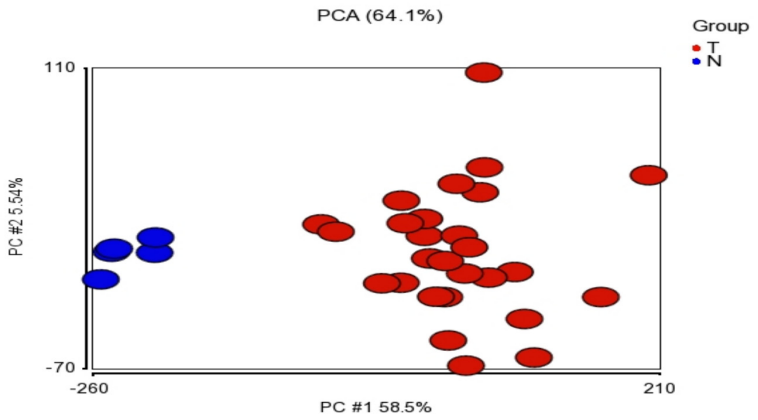

Figure 1. Differential methylation profiling in CRC tumors and adjacent normal colon samples. Principle component analysis of adjacent normal colon and CRC tumor samples. Red dots (T = tumor); blue dots (N = adjacent normal colon).

Table 2. Genome-scale analysis of DNA methylation in colorectal cancer reveals multiple hypomethylation and hypermethylation in glycolysis-related genes

Hypomethylation	Hypermethylation
ADH1A	*ALDH1A3*
ALDH7A1	*PKLR*
BPGM	
DLD	
ENO1	
G6PC2	
GAPDHS	
GCK	
HK2	
HK3	
HKDC1	
MINPP1	
PCK1	
PDHA1	
PDHA2	
PGAM2	
PGK2	

distinct clusters between pCMV6-HKDC1 and pCMV6-entry groups (**Figure 7**). A volcano plot showed that multiple genes were differentially expressed between the two groups (**Figure 7**). GSEA revealed significant up-regulation of the glycolysis pathway after *HKDC1* overexpression (**Table 3**). In addition, many cell cycle- and E2F-associated pathways were significantly upregulated in both cell types after *HKDC1* overexpression (**Table 3**). The detailed merged results of RNA sequencing and pathway analysis in the Colon320 and SW480 transfection experiments are shown in https://www.ncbi.nlm.nih.gov/geo/query/acc.cgi?acc=GSE308712, reference number GSE308712.

Discussion

In this study, we showed that hypomethylation of *HKDC1* consistently exists in four datasets (including ours) worldwide, and by manipulating *HKDC1* expression in colon cancer cells, we demonstrated that increasing *HKDC1* expression is associated with the proliferation of colon cancer cells. Thus, *HKDC1* hypomethylation may be a common epigenetic mechanism regulating cellular metabolism to promote CRC progression. HKDC1 was first identified as a conserved fifth hexokinase in various vertebrates in 2007 by Irwin and Tan [24]. Initially, a significant association between HKDC1 and 2-hour plasma glucose during pregnancy was found in a genome-wide association study [25]. Guo et al. provided functional evidence for HKDC1 in multiple cellular models and demonstrated that genetic variants in multiple regulatory elements of *HKDC1* have biological effects on glucose homeostasis [26]. Ludvik et al. found that HKDC1 plays a role in maintaining whole-body glucose use during aging and pregnancy [27]. Layden et al. found that intestinal HKDC1 can modulate the transportation of postprandial dietary glucose across the intestinal epithelium under enhanced metabolic stress [28].

HKDC1 is involved in tumorigenesis and prognosis in multiple types of cancers [29-32]. Khan et al. demonstrated the essential role of HKDC1 interaction with mitochondria in liver cancer development and progression [32]. In patients with liver cancer, high HKDC1 expression was also correlated with poor prognosis [29]. Wang et al. found that HKDC1 expression was higher in lung adenocarcinoma tissues than in adjacent normal lung tissues, and they used an in vitro model to show that HKDC1

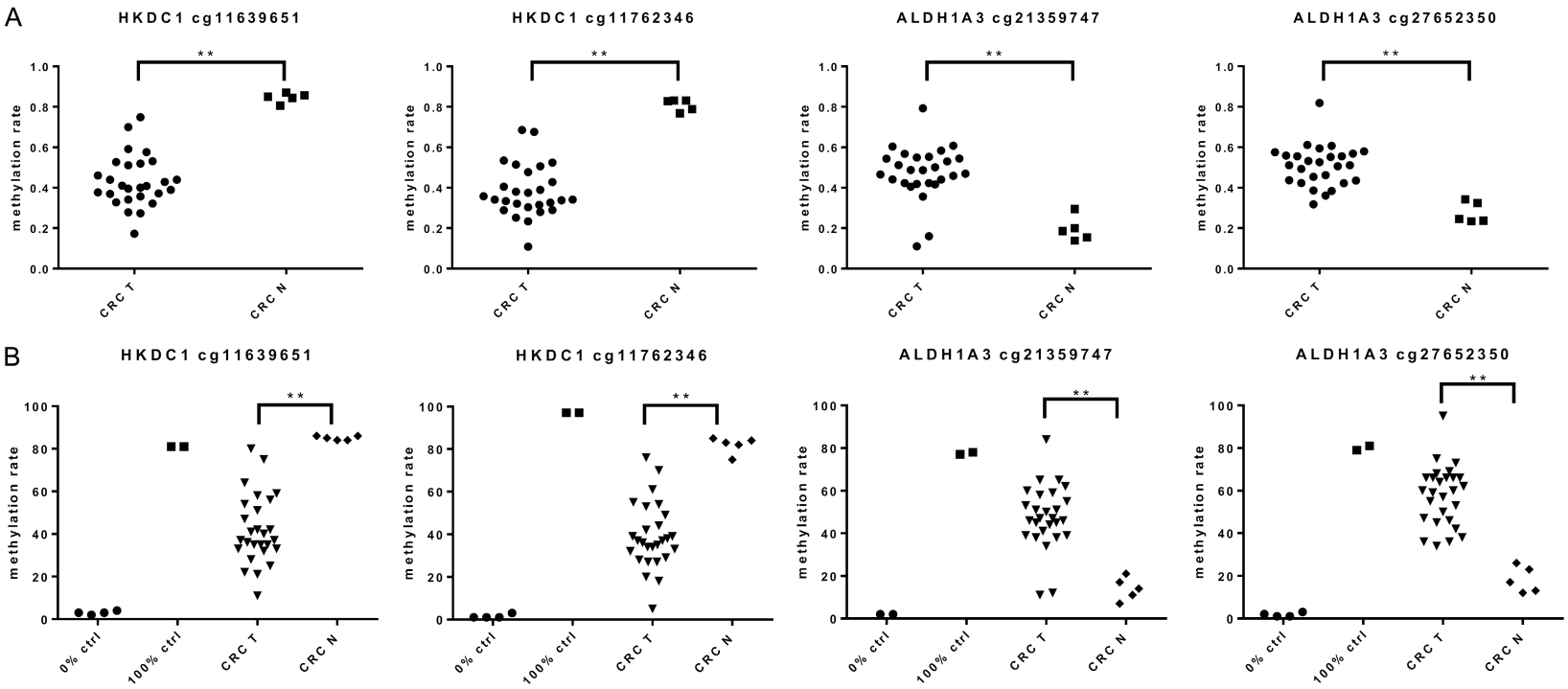

Figure 2. Validation of hypomethylated *HKDC1* and hypermethylated *ALDH1A3* by pyrosequencing. Methylation array (A) and pyrosequencing results (B). CRC T: colorectal cancer tumor; CRC N: adjacent normal colon (*$P < 0.05$, **$P < 0.01$).

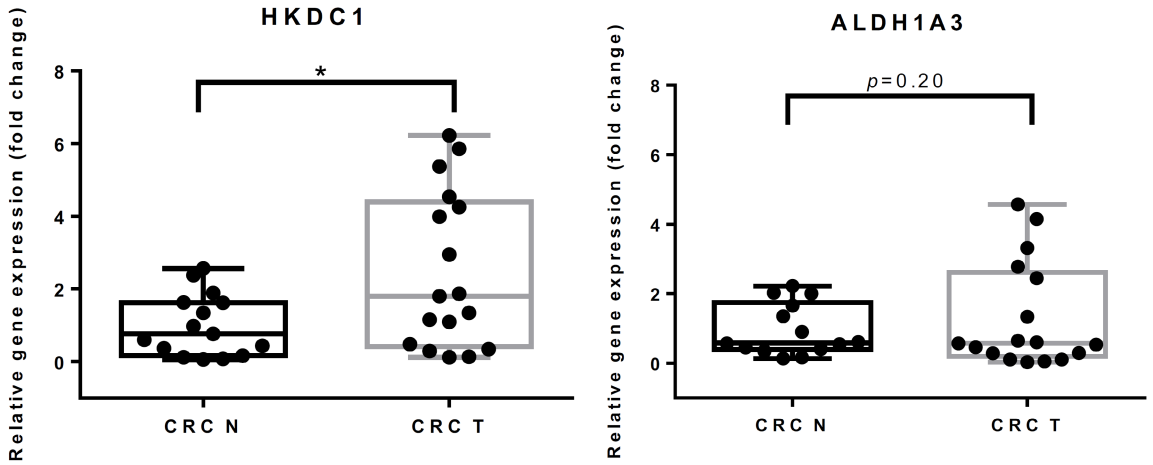

Figure 3. Relative mRNA expression of *HKDC1* and *ALDH1A3* between CRC T (colorectal cancer tumor, N = 19) and CRC N (adjacent normal colon, N = 16) by quantitative RT-PCR.

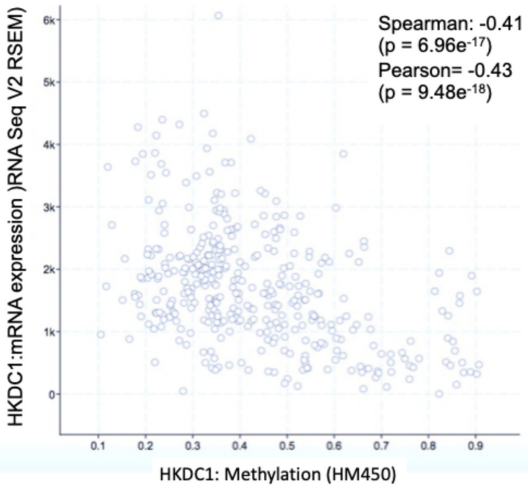

Figure 4. The association of methylation status and gene expression of *HKDC1* in CRC (C-Bioportal, TCGA, Firehose Legacy).

could promote the proliferation, invasion, and migration of lung cancer cells via the AMPK/mTOR signaling pathway [31]. In CRC, Fuhr et al. reported that *HKDC1* expression is regulated by *BMAL1,* a core clock gene, and HKDC1 expression is associated with increased glycolysis activity [30]. HKDC1 could promote CRC progression through activating Wnt/β-catenin pathway [33]. Recently, HKDC1 has also been linked to promote immune evasion in HCC models [34]. HKDC1 has also been identified as a therapeutic target in enrichment analysis of anticancer activity. In this study, we showed that an HKDC1 inhibitor (NSC24500) inhibited the proliferation of colon cancer cells. NSC24500 is also named 2,6-dimethoxy-1,4-benzoquinone and 2,6-dimethoxy-1,4-benzoquinone can be synthesized by selected lactic acid bacteria during sourdough fermentation of wheat germ [35]. Fermented wheat germ extract has been shown to inhibit glycolysis and induce apoptosis in leukemia cells *in vitro* and colon carcinogenesis *in vivo* [36, 37]. Thus, targeting HKDC1 in colon cancer warrants further study.

Cell proliferation requires energy and sufficient nutrients; thus, the cell cycle is inevitably regulated by metabolism [38]. For example, when cells are committed to entering the S phase, the expression of the glycolytic activator 6-phosphofructo-2-kinase/fructose-2,6-bisphosphatase 3 (*PFKFB3*) is essential for this process [39]. Increased glycolysis provides not only energy but also abundant glycolytic intermediates for biomass synthesis during mitosis [40]. Glycolysis can be regulated by cyclin/cyclin-dependent kinases (CDKs), retinoblastoma protein (RB), and the E2F family of transcription factors. For example, recent studies have shown that the E2F binding site is found at the 5'end of the first exon of PFKFB3 [41, 42]. Overexpression of cyclin D downregulates the expression of Hexokinase II and reduces glycolytic activity [43]. On the other hand, signaling from metabolic enzymes can regulate the progression of the cell cycle via a metabolism-independent pathway. PKM2-dependent histone H3 modifications are important for cyclin D1 expression [44]. PFKFB3 can also

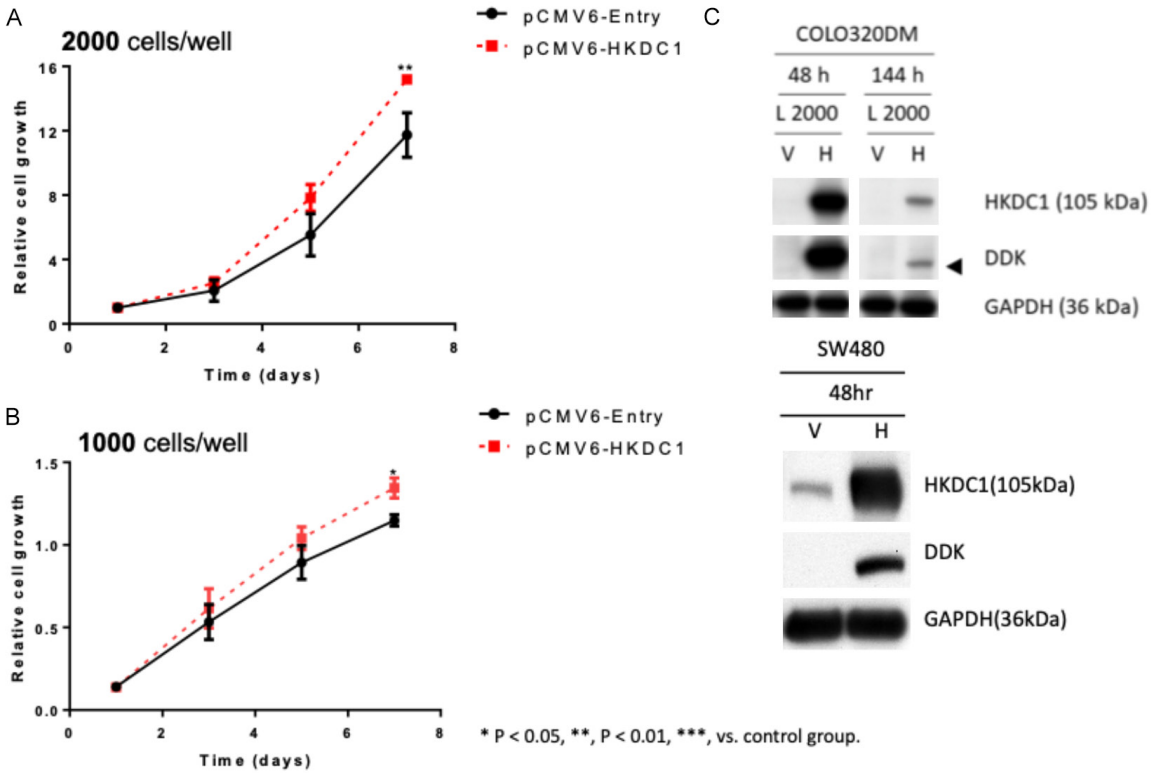

Figure 5. The increase of cell proliferation in COLO320DM and SW480 cells overexpressing *HKDC1*. The cell proliferation in *HKDC1* overexpressing (pCMV-HKDC1) group and in control (pCMV6-Entry) group in COLO320DM (A) and in SW480 cells (B) in MTT assay (**P* < 0.05, ***P* < 0.01). (C) Western blotting of HKDC1 validates *HKDC1* overexpressing in pCMV-HKDC1 (H) group in COLO320DM and SW480 cells. pCMV6-Entry (V) group is used as the control.

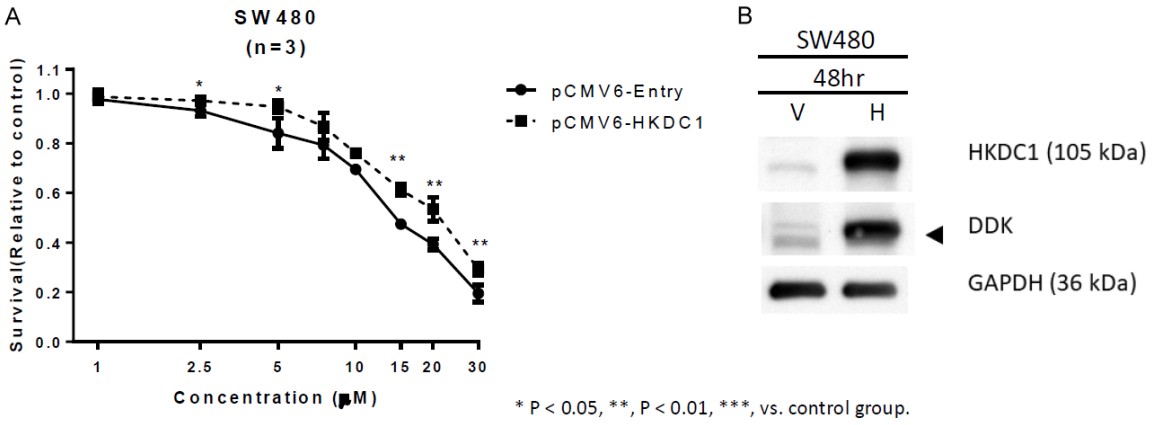

Figure 6. The decrease of drug sensitivity of SW480 cells overexpressing *HKDC1* an HKDC1 inhibitor (NSC24500) treatment. A. The cell survival is significantly increased in *HKDC1* overexpressing (pCMV-HKDC1) group than in control (pCMV6-Entry) group in SW480 cells after an HKDC1 inhibitor (NSC24500) treatment (**P* < 0.05, ***P* < 0.01). B. Western blotting of HKDC1 validates *HKDC1* overexpressing in pCMV-HKDC1 (H) group. pCMV6-Entry (V) group is used as the control. DDK: DBF4-dependent kinase.

regulate cell cycle regulators, such as upregulating cyclin D3, CDK1 and downregulating p27 [45]. Our data revealed that overexpression of another metabolic enzyme, HKDC1, upregulates the glycolysis and cell cycle pathways, probably by upregulating E2F and its targets.

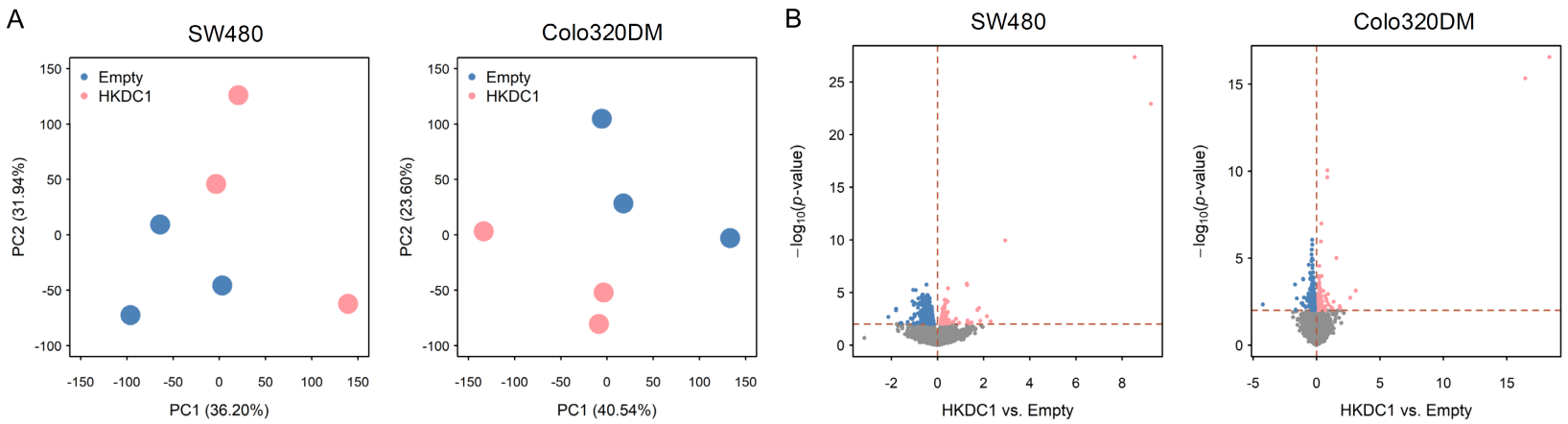

Figure 7. Differential expression profiling in *HKDC1* overexpressing (pCMV-HKDC1) group and in control (pCMV6-Entry) group in COLO320DM (A) and in SW480 cells. (A) Principle component analysis of *HKDC1* overexpressing (pCMV-HKDC1) group and control (pCMV6-Entry) group in COLO320DM (A) and in SW480 cells. Red dots (pCMV-HKDC1); blue dots (pCMV6-Entry). (B) Differential expression analysis revealed multiple genes are differentially expressed between *HKDC1* overexpressing (pCMV-HKDC1) group and control (pCMV6-Entry) group.

Table 3. Glycolysis, cell cycle, and E2F targets pathways are significantly upregulated after pCMV6-*HKDC1* transfection in both SW480 and COLO320DM cells

ID	Set Size	SW480				COLO320DM			
		Enrichment Score	NES	*p*-value	q-value	Enrichment Score	NES	*p*-value	q-value
Glycolysis									
REACTOME_GLYCOLYSIS	64	0.43	1.53	0.009	0.038	0.54	1.96	< 0.001	< 0.001
Cell cycle									
ZHOU_CELL_CYCLE_GENES_IN_IR_RESPONSE_6HR	81	0.66	2.48	< 0.001	< 0.001	0.39	1.46	0.020	0.082
ZHOU_CELL_CYCLE_GENES_IN_IR_RESPONSE_24HR	118	0.62	2.45	< 0.001	< 0.001	0.36	1.42	0.016	0.072
EGUCHI_CELL_CYCLE_RB1_TARGETS	22	0.84	2.36	< 0.001	< 0.001	0.54	1.54	0.035	0.116
WHITFIELD_CELL_CYCLE_G1_S	120	0.59	2.34	< 0.001	< 0.001	0.33	1.32	0.040	0.127
WHITFIELD_CELL_CYCLE_LITERATURE	44	0.66	2.19	< 0.001	< 0.001	0.55	1.84	< 0.001	0.007
GOBP_POSITIVE_REGULATION_OF_CELL_CYCLE_PHASE_TRANSITION	82	0.44	1.64	0.002	0.012	0.37	1.39	0.033	0.162
WHITFIELD_CELL_CYCLE_G2_M	181	0.38	1.61	< 0.001	0.002	0.36	1.53	0.001	0.010
GOBP_POSITIVE_REGULATION_OF_CELL_CYCLE_G2_M_PHASE_TRANSITION	28	0.51	1.52	0.029	0.088	0.47	1.45	0.048	0.144
E2F and its targets									
ISHIDA_E2F_TARGETS	50	0.73	2.49	< 0.001	< 0.001	0.53	1.82	< 0.001	< 0.001
HALLMARK_E2F_TARGETS	200	0.59	2.42	< 0.001	< 0.001	0.39	1.65	< 0.001	0.002
KALMA_E2F1_TARGETS	11	0.8	1.9	< 0.001	< 0.001	0.64	1.53	0.041	0.130
BILD_E2F3_ONCOGENIC_SIGNATURE	213	0.41	1.74	< 0.001	< 0.001	0.33	1.43	0.005	0.034
IGLESIAS_E2F_TARGETS_UP	100	0.36	1.39	0.023	0.075	0.35	1.33	0.047	0.142

This study had several limitations. First, the platforms of the methylation array used in the open datasets were not the same, and we may not have identified all shared significant DMGs that are involved in the glycolysis pathway [21-23]. However, to our knowledge, our study is the first to show that hypomethylation of *HKDC1* is a shared DMG in colon cancer. Second, we could not manipulate the methylation status of *HKDC1* specifically in colon cancer cells; thus, we overexpressed *HKDC1* to mimic the increased expression of *HKDC1* under hypomethylated conditions. The rationale for this alternative experiment was that our data support that *HKDC1* expression is regulated by methylation in colorectal cancer.

In conclusion, we identified that hypomethylation of *HKDC1* is a shared differentially methylated gene in CRC, and *HKDC1* expression is methylation-regulated. Our data revealed that hypomethylation of *HKDC1* may be one of the mechanisms regulating cellular metabolism to promote proliferation of colon cancer cells, probably through the upregulation of glycolysis and cell cycle pathways.

Acknowledgements

The authors thank the National Center for High-performance Computing (NCHC) for providing computational and storage resources, and the High-Throughput Genomics and Big Data Analysis Core, Department of Medical Research, National Taiwan University Hospital, for providing the analysis facilities. This work was supported by the National Science and Technology Council under the Grant (number 107-2314-B-002-204-MY2).

Disclosure of conflict of interest

None.

Address correspondence to: Dr. Kun-Huei Yeh, Department of Oncology, National Taiwan University Hospital, No. 7, Chung-Shan South Road, Taipei 10002, Taiwan. Tel: +886-2-23123456 Ext. 66285; Fax: +886-2-23711174; E-mail: khyeh@ntu.edu.tw

References

[1] Sung H, Ferlay J, Siegel RL, Laversanne M, Soerjomataram I, Jemal A and Bray F. Global Cancer Statistics 2020: GLOBOCAN estimates of incidence and mortality worldwide for 36 cancers in 185 countries. CA Cancer J Clin 2021; 71: 209-249.

[2] Taiwan Cancer Registry Annual Report 2019.

[3] Le Marchand L, Wilkens LR, Kolonel LN, Hankin JH and Lyu LC. Associations of sedentary lifestyle, obesity, smoking, alcohol use, and diabetes with the risk of colorectal cancer. Cancer Res 1997; 57: 4787-4794.

[4] Slattery ML, Edwards SL, Boucher KM, Anderson K and Caan BJ. Lifestyle and colon cancer: an assessment of factors associated with risk. Am J Epidemiol 1999; 150: 869-877.

[5] Johnson CM, Wei C, Ensor JE, Smolenski DJ, Amos CI, Levin B and Berry DA. Meta-analyses of colorectal cancer risk factors. Cancer Causes Control 2013; 24: 1207-1222.

[6] Hanahan D and Weinberg RA. Hallmarks of cancer: the next generation. Cell 2011; 144: 646-674.

[7] Warburg O. On the origin of cancer cells. Science 1956; 123: 309-314.

[8] Finley LWS and Thompson CB. The metabolism of cell growth and proliferation. The Molecular Basis of Cancer (Fourth Edition) 2015; 191-208.

[9] Miyamoto S, Murphy AN and Brown JH. Akt mediates mitochondrial protection in cardiomyocytes through phosphorylation of mitochondrial hexokinase-II. Cell Death Differ 2008; 15: 521-529.

[10] Yun J, Rago C, Cheong I, Pagliarini R, Angenendt P, Rajagopalan H, Schmidt K, Willson JK, Markowitz S, Zhou S, Diaz LA Jr, Velculescu VE, Lengauer C, Kinzler KW, Vogelstein B and Papadopoulos N. Glucose deprivation contributes to the development of KRAS pathway mutations in tumor cells. Science 2009; 325: 1555-1559.

[11] Morani F, Phadngam S, Follo C, Titone R, Aimaretti G, Galetto A, Alabiso O and Isidoro C. PTEN regulates plasma membrane expression of glucose transporter 1 and glucose uptake in thyroid cancer cells. J Mol Endocrinol 2014; 53: 247-258.

[12] Klose RJ and Bird AP. Genomic DNA methylation: the mark and its mediators. Trends Biochem Sci 2006; 31: 89-97.

[13] Lopez-Serra P, Marcilla M, Villanueva A, Ramos-Fernandez A, Palau A, Leal L, Wahi JE, Setien-Baranda F, Szczesna K, Moutinho C, Martinez-Cardus A, Heyn H, Sandoval J, Puertas S, Vidal A, Sanjuan X, Martinez-Balibrea E, Vinals F, Perales JC, Bramsem JB, Orntoft TF, Andersen CL, Tabernero J, McDermott U, Boxer MB, Vander Heiden MG, Albar JP and Esteller M. A DERL3-associated defect in the degradation of SLC2A1 mediates the Warburg effect. Nat Commun 2014; 5: 3608.

[14] Desai S, Ding M, Wang B, Lu Z, Zhao Q, Shaw K, Yung WK, Weinstein JN, Tan M and Yao J.

Tissue-specific isoform switch and DNA hypomethylation of the pyruvate kinase PKM gene in human cancers. Oncotarget 2014; 5: 8202-8210.

[15] Hughes LA, van den Brandt PA, Goldbohm RA, de Goeij AF, de Bruine AP, van Engeland M and Weijenberg MP. Childhood and adolescent energy restriction and subsequent colorectal cancer risk: results from the Netherlands Cohort Study. Int J Epidemiol 2010; 39: 1333-1344.

[16] Lea AJ, Altmann J, Alberts SC and Tung J. Resource base influences genome-wide DNA methylation levels in wild baboons (Papio cynocephalus). Mol Ecol 2016; 25: 1681-1696.

[17] Bollati V and Baccarelli A. Environmental epigenetics. Heredity (Edinb) 2010; 105: 105-112.

[18] Chen KH, Lin LI, Yuan CT, Tseng LH, Chao YL, Liang YH, Liang JT, Lin BR, Cheng AL and Yeh KH. Association between risk factors, molecular features and CpG island methylator phenotype colorectal cancer among different age groups in a Taiwanese cohort. Br J Cancer 2021; 125: 48-54.

[19] Bolger AM, Lohse M and Usadel B. Trimmomatic: a flexible trimmer for Illumina sequence data. Bioinformatics 2014; 30: 2114-2120.

[20] Kim D, Langmead B and Salzberg SL. HISAT: a fast spliced aligner with low memory requirements. Nat Methods 2015; 12: 357-360.

[21] Naumov VA, Generozov EV, Zaharjevskaya NB, Matushkina DS, Larin AK, Chernyshov SV, Alekseev MV, Shelygin YA and Govorun VM. Genome-scale analysis of DNA methylation in colorectal cancer using Infinium HumanMethylation450 BeadChips. Epigenetics 2013; 8: 921-934.

[22] Hinoue T, Weisenberger DJ, Lange CP, Shen H, Byun HM, Van Den Berg D, Malik S, Pan F, Noushmehr H, van Dijk CM, Tollenaar RA and Laird PW. Genome-scale analysis of aberrant DNA methylation in colorectal cancer. Genome Res 2012; 22: 271-282.

[23] Cancer Genome Atlas Network. Comprehensive molecular characterization of human colon and rectal cancer. Nature 2012; 487: 330-337.

[24] Irwin DM and Tan H. Molecular evolution of the vertebrate hexokinase gene family: Identification of a conserved fifth vertebrate hexokinase gene. Comp Biochem Physiol Part D Genomics Proteomics 2008; 3: 96-107.

[25] Hayes MG, Urbanek M, Hivert MF, Armstrong LL, Morrison J, Guo C, Lowe LP, Scheftner DA, Pluzhnikov A, Levine DM, McHugh CP, Ackerman CM, Bouchard L, Brisson D, Layden BT, Mirel D, Doheny KF, Leya MV, Lown-Hecht RN, Dyer AR, Metzger BE, Reddy TE, Cox NJ and Lowe WL Jr; HAPO Study Cooperative Research Group. Identification of HKDC1 and BACE2 as genes influencing glycemic traits during pregnancy through genome-wide association studies. Diabetes 2013; 62: 3282-3291.

[26] Guo C, Ludvik AE, Arlotto ME, Hayes MG, Armstrong LL, Scholtens DM, Brown CD, Newgard CB, Becker TC, Layden BT, Lowe WL and Reddy TE. Coordinated regulatory variation associated with gestational hyperglycaemia regulates expression of the novel hexokinase HKDC1. Nat Commun 2015; 6: 6069.

[27] Ludvik AE, Pusec CM, Priyadarshini M, Angueira AR, Guo C, Lo A, Hershenhouse KS, Yang GY, Ding X, Reddy TE, Lowe WL Jr and Layden BT. HKDC1 is a novel hexokinase involved in whole-body glucose use. Endocrinology 2016; 157: 3452-3461.

[28] Zapater JL, Wicksteed B and Layden BT. Enterocyte HKDC1 modulates intestinal glucose absorption in male mice fed a high-fat diet. Endocrinology 2022; 163: bqac050.

[29] Zhang Z, Huang S, Wang H, Wu J, Chen D, Peng B and Zhou Q. High expression of hexokinase domain containing 1 is associated with poor prognosis and aggressive phenotype in hepatocarcinoma. Biochem Biophys Res Commun 2016; 474: 673-679.

[30] Fuhr L, El-Athman R, Scrima R, Cela O, Carbone A, Knoop H, Li Y, Hoffmann K, Laukkanen MO, Corcione F, Steuer R, Meyer TF, Mazzoccoli G, Capitanio N and Relogio A. The circadian clock regulates metabolic phenotype rewiring via HKDC1 and modulates tumor progression and drug response in colorectal cancer. EBioMedicine 2018; 33: 105-121.

[31] Wang X, Shi B, Zhao Y, Lu Q, Fei X, Lu C, Li C and Chen H. HKDC1 promotes the tumorigenesis and glycolysis in lung adenocarcinoma via regulating AMPK/mTOR signaling pathway. Cancer Cell Int 2020; 20: 450.

[32] Khan MW, Terry AR, Priyadarshini M, Ilievski V, Farooq Z, Guzman G, Cordoba-Chacon J, Ben-Sahra I, Wicksteed B and Layden BT. The hexokinase "HKDC1" interaction with the mitochondria is essential for liver cancer progression. Cell Death Dis 2022; 13: 660.

[33] Huang S, Pang Q, Zhang Y and Cao J. HKDC1 promotes colorectal cancer progression by regulating RCOR1 expression to activate the Wnt/β-catenin pathway, enhancing proliferation, migration, and epithelial-mesenchymal transition. J Biol Chem 2025; 301: 108478.

[34] Zhang Y, Wang M, Ye L, Shen S, Zhang Y, Qian X, Zhang T, Yuan M, Ye Z, Cai J, Meng X, Qiu S, Liu S, Liu R, Jia W, Yang X, Zhang H, Zhong X and Gao P. HKDC1 promotes tumor immune evasion in hepatocellular carcinoma by cou-

pling cytoskeleton to STAT1 activation and PD-L1 expression. Nat Commun 2024; 15: 1314.
[35] Rizzello CG, Mueller T, Coda R, Reipsch F, Nionelli L, Curiel JA and Gobbetti M. Synthesis of 2-methoxy benzoquinone and 2,6-dimethoxybenzoquinone by selected lactic acid bacteria during sourdough fermentation of wheat germ. Microb Cell Fact 2013; 12: 105.
[36] Zalatnai A, Lapis K, Szende B, Rásó E, Telekes A, Resetár A and Hidvégi M. Wheat germ extract inhibits experimental colon carcinogenesis in F-344 rats. Carcinogenesis 2001; 22: 1649-1652.
[37] Comin-Anduix B, Boros LG, Marin S, Boren J, Callol-Massot C, Centelles JJ, Torres JL, Agell N, Bassilian S and Cascante M. Fermented wheat germ extract inhibits glycolysis/pentose cycle enzymes and induces apoptosis through poly(ADP-ribose) polymerase activation in Jurkat T-cell leukemia tumor cells. J Biol Chem 2002; 277: 46408-46414.
[38] Kalucka J, Missiaen R, Georgiadou M, Schoors S, Lange C, De Bock K, Dewerchin M and Carmeliet P. Metabolic control of the cell cycle. Cell Cycle 2015; 14: 3379-3388.
[39] Tudzarova S, Colombo SL, Stoeber K, Carcamo S, Williams GH and Moncada S. Two ubiquitin ligases, APC/C-Cdh1 and SKP1-CUL1-F (SCF)-beta-TrCP, sequentially regulate glycolysis during the cell cycle. Proc Natl Acad Sci U S A 2011; 108: 5278-5283.
[40] Lunt SY and Vander Heiden MG. Aerobic glycolysis: meeting the metabolic requirements of cell proliferation. Annu Rev Cell Dev Biol 2011; 27: 441-464.
[41] Darville MI, Antoine IV, Mertens-Strijthagen JR, Dupriez VJ and Rousseau GG. An E2F-dependent late-serum-response promoter in a gene that controls glycolysis. Oncogene 1995; 11: 1509-1517.
[42] Darville MI and Rousseau GG. E2F-dependent mitogenic stimulation of the splicing of transcripts from an S phase-regulated gene. Nucleic Acids Res 1997; 25: 2759-2765.
[43] Sakamaki T, Casimiro MC, Ju X, Quong AA, Katiyar S, Liu M, Jiao X, Li A, Zhang X, Lu Y, Wang C, Byers S, Nicholson R, Link T, Shemluck M, Yang J, Fricke ST, Novikoff PM, Papanikolaou A, Arnold A, Albanese C and Pestell R. Cyclin D1 determines mitochondrial function in vivo. Mol Cell Biol 2006; 26: 5449-5469.
[44] Yang W, Xia Y, Hawke D, Li X, Liang J, Xing D, Aldape K, Hunter T, Alfred Yung WK and Lu Z. PKM2 phosphorylates histone H3 and promotes gene transcription and tumorigenesis. Cell 2012; 150: 685-696.
[45] Yalcin A, Clem BF, Simmons A, Lane A, Nelson K, Clem AL, Brock E, Siow D, Wattenberg B, Telang S and Chesney J. Nuclear targeting of 6-phosphofructo-2-kinase (PFKFB3) increases proliferation via cyclin-dependent kinases. J Biol Chem 2009; 284: 24223-24232.

Supplementary Table 1. The methylation percentage of *HKDC1* and *ALDH1A3* in each sample in pyrosequencing

Sample	HKDC1		ALDH1A3	
	Cg11762346	Cg11639651	Cg27652350	Cg21359747
CRC095N	83	84	13	11
CRC105N	82	86	23	17
CRC106N	84	84	17	14
CRC118N	75	85	26	21
CRC141N	85	86	12	7
CRC088	55	58	36	38
CRC091	44	47	64	47
CRC095	34	37	68	62
CRC096	37	42	60	55
CRC097	76	80	55	41
CRC098	61	64	36	34
CRC099	29	32	66	51
CRC102	70	75	42	44
CRC105	38	37	60	38
CRC106	18	22	45	46
CRC107	28	35	73	65
CRC109	35	36	34	12
CRC112	34	33	66	51
CRC113	33	33	69	59
CRC115	27	25	75	45
CRC116	53	56	62	45
CRC117	39	40	66	53
CRC118	49	51	46	50
CRC125	32	35	66	60
CRC127	36	42	53	58
CRC128	27	28	38	11
CRC129	37	35	47	65
CRC134	20	21	50	39
CRC137	39	41	57	39
CRC139	42	59	66	46
CRC140	54	54	59	47
CRC141	5	11	95	84
0%	1, 3, 1, 1	2, 3, 4, 3	1, 3, 1, 2	2, 2
100%	97, 97	81, 81	79, 81	77, 78

Supplementary Table 2. The methylation percentage of *HKDC1* in six colon cancer cells by pyrosequencing

HKDC1 methylation		
Loci	cg11762346	cg11639651
Sample	Methylation (%)*	Methylation (%)*
COLO205	2.99	2,24
COLO320	77.21	71.38
SW480	43.97	67.80
SW620	10.84	54.54
HCT15	68.99	82.74
HT29	5.76	16.95

*Mean of four independent experiments.

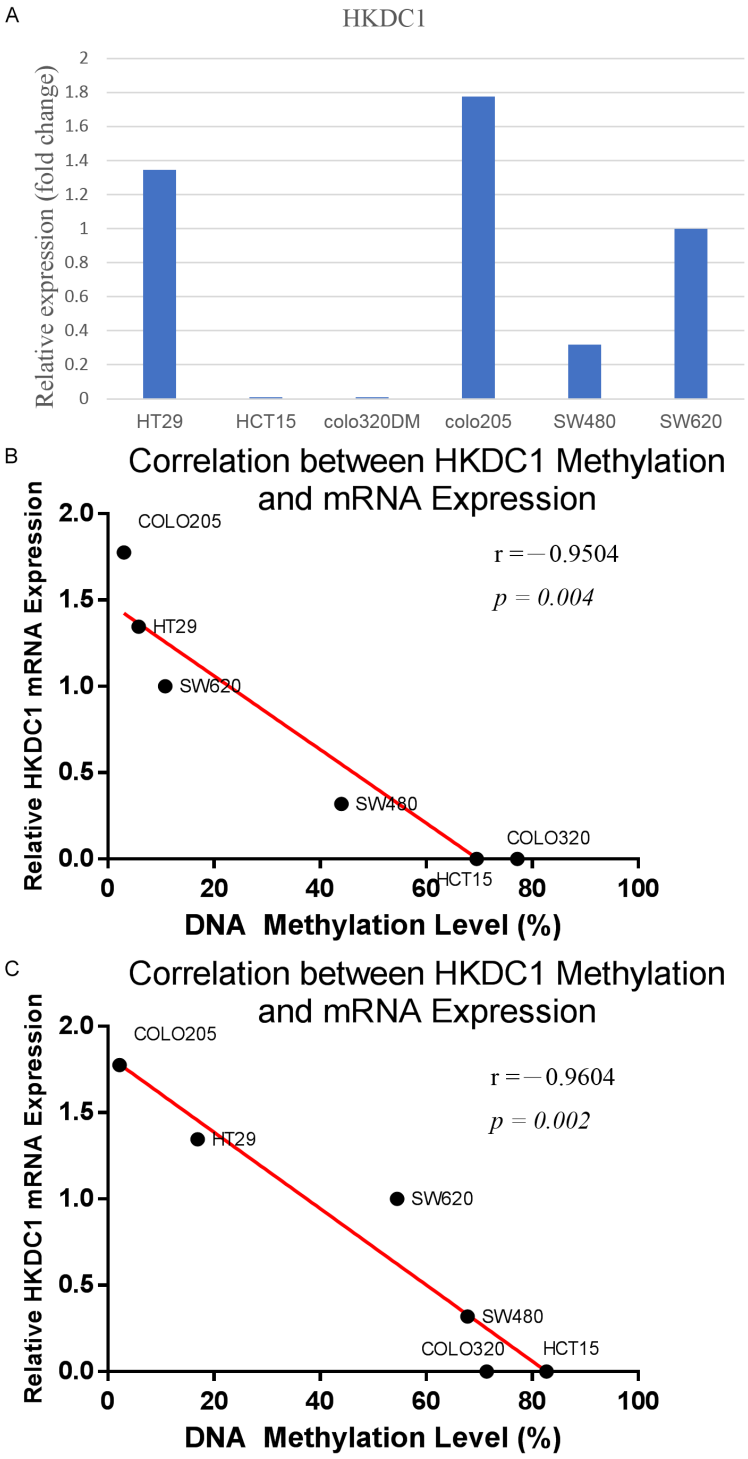

Supplementary Figure 1. (A) Relative mRNA expression of *HKDC1* between six colon cancer cell lines by quantitative RT-PCR. The association of *HKDC1* methylation status based on (B) cg11762346 and cg11639651 (C) and mRNA expression of *HDKC1* in six colon cancer cells.

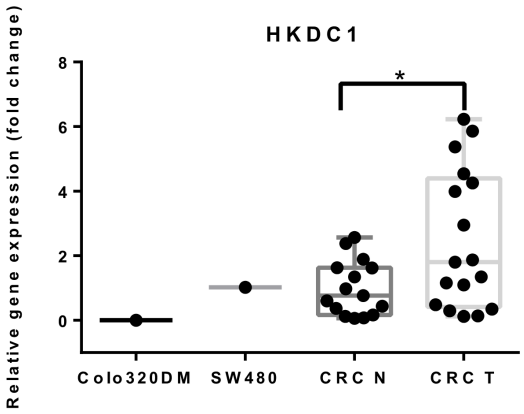

Supplementary Figure 2. Relative mRNA expression of *HKDC1* between CRC T (colorectal cancer tumor, N = 19), CRC N (adjacent normal colon, N = 16), and two colon cancer cell lines by quantitative RT-PCR.

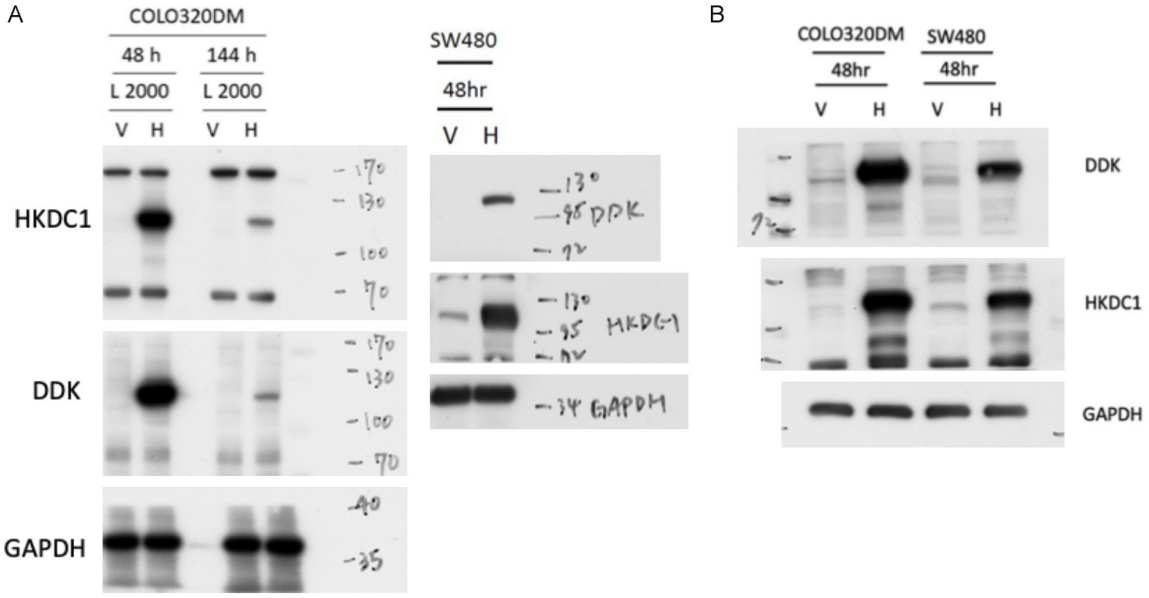

Supplementary Figure 3. (.pptx): The full uncropped gel and blot image(s) of HKDC1 transfection in COLO320DM and SW480 cells in **Figures 5A** and **6B**.